In-situ capacitive sensor for monitoring debris of lubricant oil

Yishou Wang, Zhibin Han, Tian Gao and Xinlin Qing
Xiamen University, Xiamen, China

Abstract

Purpose – The purpose of this study is to develop a cylindrical capacitive sensor that has the advantages of high resolution, small size and designability and can be easily installed on lubricant pipeline to monitor lubricant oil debris.

Design/methodology/approach – A theoretical model of the cylindrical capacitive sensor is presented to analyze several parameters' effectiveness on the performance of sensor. Numerical simulations are then conducted to determine the optimal parameters for preliminary experiments. Experiments are finally carried out to demonstrate the detectability of developed capacitive sensors.

Findings – It is clear from experimental results that the developed capacitive sensor can monitor the debris in lubricant oil well, and the capacitance values increase almost linearly when the number and size of debris increase.

Research limitations/implications – There is lot of further work to do to apply the presented method into the application. Especially, it is necessary to consider several factors' influence on monitoring results. These factors include the flow rate of the lubricant oil, the temperature, the debris distribution and the vibration. Moreover, future work should consider the influence of the oil degradation to the capacitance change and other contaminations (e.g. water and dust).

Practical implications – This work conducts a feasibility study on application of capacitive sensing principle for detecting debris in aero engine lubricant oil.

Originality/value – The novelty of the presented capacitance sensor can be summarized into two aspects. One is that the sensor structure is simple and characterized by two coaxial cylinders as electrodes, while conventional capacitive sensors are composed of two parallel plates as electrodes. The other is that sensing mechanism and physical model of the presented sensor is verified and validated by the simulation and experiment.

Keywords Lubricant oil, Capacitive sensor, Debris monitoring, Engine health monitoring

Paper type Research paper

1. Introduction

Aircraft engine, as a core component, is directly related to the performance and safety of aircraft. The continuous flowing lubricant oil is used to not only reduce the temperature but also transport the debris/particles produced by mechanical wear. The debris not only affects the performance of lubricant oil but also indicates some states of the mechanical system in the engine. The wear particles in lubrication oil maintain a constant concentration and small size in normal working conditions; however, when abnormal wear occurs, the concentration and sizes of the particles increase and are distinct from normal particles (Mauntz *et al.*, 2013). Therefore, the detection of lubricant oil debris (size and concentration) is an important and effective method for fault diagnosis and life prediction of key components in engine.

Several attempts have been made in the past decade to detect the conditions of lubricant oil. Laboratory (offline) and *in situ* (online) methods are both used in metal particle analysis. The offline approaches depend on skillful sampling, a diagnostic database and a long period; these include ferrography (Matsumoto *et al.*, 2016) and spectrometric analysis (Guan *et al.*, 2011). The continuous online health monitoring of engine is an important way to ensure its stability and reliability in the service. *In situ* monitoring of lubricant oil quality has become an important issue in today's military, transportation and manufacturing industries (Jaw, 2005).

Online lubricant oil condition detection methods include optical detection (Iwai *et al.*, 2010), photoelectric and magnetic hybrid detection (Kuo *et al.*, 1997), inductive/ detection (Wu *et al.*, 2016; Hong *et al.*, 2015), capacitance detection (Minasamudram *et al.*, 2013; Appleby *et al.*, 2013; Ding *et al.*, 2012), ultrasonic/acoustic detection (Xu *et al.*, 2015), electrical impedance detection (Itomi, 2006), online x-ray spectrography

The current issue and full text archive of this journal is available on Emerald Insight at: **www.emeraldinsight.com/0036-8792.htm**

Industrial Lubrication and Tribology
70/7 (2018) 1310–1319
Emerald Publishing Limited [ISSN 0036-8792]
[DOI 10.1108/ILT-09-2017-0256]

The authors would like to acknowledge the financial support of the National Natural Science Foundation of China (Grants No. 11472308, 51475067). The authors also would like to thank the support of and the Fundamental Research Funds for the Central Universities (20720170123).

Received 12 September 2017
Revised 14 December 2017
Accepted 11 January 2018

(Kayani, 2009) and electrostatic charge detection (Powrie, 2000). Advantages and disadvantages of all these online condition monitoring technologies have been listed in the literature (Du and Zhe, 2011). Wu *et al.* (2013) comprehensively reviewed the progress of online oil monitoring techniques, mainly focusing on sensor technologies, their scopes and industrial applications. Generally, if these online methods are really applied in monitoring the lubricant oil of complex aircraft engine, some challenges should be solved, such as environmental compensation, compatibility with structures and electromagnetic property, high reliability and robustness, high resolution and accuracy for weak and random signals.

To remedy the limitation of a single method, many researchers have proposed some integrated approaches to play their own advantages. For example, Appleby *et al.* (2013) combine ultrasonic, capacitance and inductance-based methods detect oil debris contents and analyze other physical parameters associated with lubricating oil degradation. Matsumoto *et al.* (2016) presented a hybrid approach combining scanning electron microscope and ferrography to observe the wear debris particles in lubricant oil during stable wear state and abnormal wear state. Xu *et al.* (2015) adopted the matching pursuit and quantum-behaved particle swarm optimization to extract the ultrasonic echo wave shape features that can distinguish the debris with different shapes and air bubble. Some useful apparatuses have been developed by microfluidic techniques that can detect the individual particles according to different principles (Zhang *et al.*, 2009). These devices include the resistive pulse sensor, capacitance counter sensor and inductive counter sensors (Du *et al.*, 2010).

Capacitive sensors have been widely used because of its good temperature stability, simple structure, strong adaptability, good dynamic response, noncontact measurement and other advantages (Stevan *et al.*, 2015). Although the capacitance methods have some problems, such as sensitive to oil quality, they are still the most practical and effective methods in many applications (Aslam and Tang, 2014; Dong and Barbosa, 2015). Generally, the capacitive sensors can be divided into three kinds such as the dielectric constant, the distance between two electrodes and the common area between two electrode surfaces. Therefore, this study designs an *in situ* capacitive sensor for monitoring debris of engine lubricant oil. The basic principle is that the debris gets into the oil and lead to the change of the dielectric constant of oil, which will lead to the change of capacitance. Hence, we can use the capacitance change to characterize whether the oil contains debris or not. The novelty of the presented capacitance sensor can be summarized as two aspects. One is that the sensor structure is simple and characterized by two coaxial cylinders as electrodes, while conventional capacitive sensors are composed of two parallel plates as electrodes. This structure feature is beneficial to easy integration with oil pipeline. The other is that sensing mechanism and physical model of the presented sensor is verified and validated by the simulation and experiment.

The aim of this work is to conduct a feasibility study on application of capacitive sensing principle for detecting debris in lubricant oil. The remained paper is organized as follows. First, the theoretical model of capacitive sensor is developed to analyze key parameters. Next, a detailed process of the numerical simulation is presented together with the results. Finally, the preliminary experimental results are presented and key conclusions are drawn.

2. Structure and math model of capacitive sensor

2.1 Sensor structure

A capacitive sensor is a device whose physical characteristics determine the value of its capacitance. These characteristics include the distance between two electrodes, the common surface and the dielectric element, as shown in Figure 1. To the authors' knowledge, the most structures of capacitive sensors is plate-like with the same or similar area (Stevan *et al.*, 2015).

Considering that the lubricant oil pipeline is small in diameter, this study designs a coaxial capacitive sensor and its structure is shown in Figure 2(a). It includes three components: the outer core, the inner core and the connector or joint. The connector is used not only to fix two cores but also to integrate with the original pipeline. The whole assembly scheme is illustrated as shown in Figure 2(b). It is obviously seen that the presented structure is simple and easily installed on the lubricant oil pipeline. The joint can be designed as a connecting flange or a nut of two pipelines (the detailed design described in Section 4). Lubricant oil flows through an annular space between the outer core and the inner core. If there is no debris in the oil, the dielectric constant between two poles is stable in value. That is to say that the measured capacitance will not be changed. When the oil contains debris, the value of the dielectric constant between two poles is changed, which will result in the capacitance change.

2.2 Mathematical model

The capacitance of the sensor depends on the dielectric permittivity of medium between the pair of electrodes. For a conventional parallel capacitive sensor, it is easy to calculate the capacitance (C) between the two parallel plates (electrodes) of a capacitor according the formula described in the Ref (Stevan *et al.*, 2015).

To establish a mathematical model for a capacitive sensor as shown in Figure 3(a), this study presents some assumptions as follows: The inner core is simplified as a long uniform charged rod with radius R_1, so the electric field in the sensor can be analyzed through the field distribution in a uniformly charged thin rod; the thickness of the outer core is not only considered but also regarded as a curved surface with radius R_2. Because of the symmetry of the sensor structure, the model can be simplified from three-dimensional space to two-dimensional plane as shown in Figure 3(b). Take any point O in a thin rod as the coordinate origin to establish coordinate system whose x axis is along the inner core, while y axis is perpendicular to the inner core. Set any point outside the rod as Q, whose distance to the thin rod is d, and the angles between the x axis and two lines from Q to two endpoints of the thin rod are illustrated by a_1 and a_2, respectively. Finally, the linear charge density is set as η_e. The relative parameters of the mathematical model are shown in Figure 3(b).

Take a line element dx whose charge is $dq = \eta_e dx$ at the position x. The intensity of the electric field generated by dq in Q point is defined as Formula (1):

Figure 1 Schematic diagram of conventional capacitive sensor structure

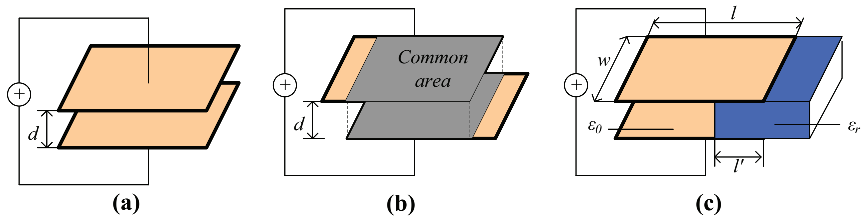

Notes: (a) Variation in the distance between the plates; (b) variation of the common surface; (c) change of the dielectric element

Figure 2 Schematic diagram of the presented capacitive sensor model

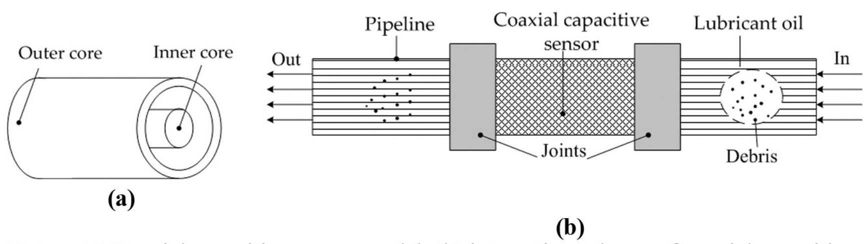

Notes: (a) Coaxial capacitive sensor model; (b) integration scheme of coaxial capacitive sensor and lubricant oil pipeline

Figure 3 Simplified model of capacitive sensor

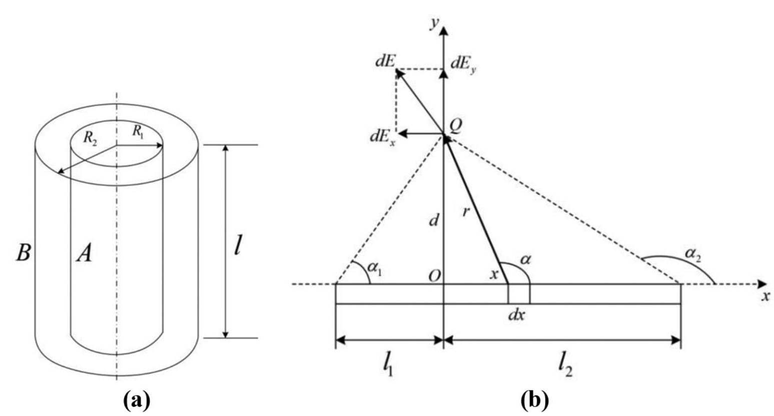

Notes: (a) 3D Illustration and its size of capacitive sensor; (b) the parameters illustration of 2D capacitive sensor

$$dE = \frac{1}{4\pi\varepsilon_0}\frac{dq}{r^2} = \frac{\eta_e}{4\pi\varepsilon_0}\frac{dx}{r^2} \tag{1}$$

The line element dq in different positions of the thin rod will produce different element field dE at the position Q. To illustrate the whole electric field, we have to decompose vector dE along two axes and get that:

$$\begin{cases} dE_x = dE\cos\alpha = \dfrac{1}{4\pi\varepsilon_0}\dfrac{\eta_e dx}{r^2}\cos\alpha \\ dE_y = dE\sin\alpha = \dfrac{1}{4\pi\varepsilon_0}\dfrac{\eta_e dx}{r^2}\sin\alpha \end{cases} \tag{2}$$

With the equation (2), the electric field intensity produced by each line element at x axis and y axis can be expressed as equation (3):

$$\begin{cases} E_x = \int dE_x = \int \dfrac{1}{4\pi\varepsilon_0}\dfrac{\eta_e dx}{r^2}\cos\alpha = \dfrac{\eta_e}{4\pi\varepsilon_0 d}\displaystyle\int_{\alpha_1}^{\alpha_2}\cos\alpha d\alpha = \dfrac{\eta_e}{4\pi\varepsilon_0 d}(\sin\alpha_1 - \sin\alpha_2) \\ E_y = \int dE_y = \int \dfrac{1}{4\pi\varepsilon_0}\dfrac{\eta_e dx}{r^2}\sin\alpha = \dfrac{\eta_e}{4\pi\varepsilon_0 d}\displaystyle\int_{\alpha_1}^{\alpha_2}\sin\alpha d\alpha = \dfrac{\eta_e}{4\pi\varepsilon_0 d}(\cos\alpha_1 - \cos\alpha_2) \end{cases} \tag{3}$$

According to the equation (3), we can calculate the values of E_x and E_y. If we change the values of two parameters d and l, the entire field distribution will be different. There are two cases should be discussed. In this research, the d is far smaller than l, we just consider the condition that $d \ll l$.

When $d \ll l$, the thin rod can be arbitrarily long, that is, $\alpha_1 = 0$, $\alpha_2 = \pi$. We can obtain the equation (4):

$$\begin{cases} E_x = 0 \\ E_y = \dfrac{\eta_e}{2\pi\varepsilon_0 d} \end{cases} \tag{4}$$

In this study, the diameter of oil pipeline is small, so the physical model of the cylindrical capacitive sensor is much closer to the first case. In the process of above analysis, ε_0 is a vacuum dielectric constant. However, the dielectric constant in the actual situation is not equal to ε_0. Therefore, this study introduces a parameter ε_r defined as relative dielectric constant. Then the actual dielectric constant can be formulated as $\varepsilon = \varepsilon_0\varepsilon_r$. Hence, the formula (4) can be further rewritten as follows:

$$E = \frac{\eta_e}{2\pi\varepsilon_0\varepsilon_r r} = \frac{q}{2\pi\varepsilon_0\varepsilon_r l}\frac{1}{r} \tag{5}$$

In equation (5), q is the quantity of the electric charge of the cylinder, l is the length of cylinder. Then $\eta_e = q/l$. The cylinder capacitive sensor is made of two coaxial metal cylinders A and B with radiuses R_1 and R_2, respectively. The length of cylinders l is much larger than R_1. The ε_r is dielectric constant between two cylinders. As shown in Figure 2, the direction of the electric field is perpendicular to the axis of the cylinder. Then the electric potential difference between two surfaces of two cylinders can be obtained by Formula (6):

$$V_{AB} = \int_l E \cdot dr = \int_{R_1}^{R_2} \frac{q}{2\pi\varepsilon_0\varepsilon_r l}\frac{dr}{r} = \frac{q}{2\pi\varepsilon_0\varepsilon_r l}\ln\frac{R_2}{R_1} \tag{6}$$

The capacitance is calculated by the following equation (7):

$$C = \frac{q}{V_{AB}} = \frac{2\pi\varepsilon_0\varepsilon_r l}{\ln\frac{R_2}{R_1}} \tag{7}$$

According to above formula (7), we can see that the capacitance C is a function of l, ε_r and $\ln(R_2/R_1)$. Therefore, if l and $\ln(R_2/R_1)$ are known constant, C is just a function of ε_r. When there is a debris particle passing through the sensor, this debris particle can be seen as an electric dipole. So, the problem can be simplified as the polarization of the dielectric under an external electric field E_0. The polarization charge appears on the surface of the dielectric and generates an additional electric field E', so the field intensity E at any point in the space is equal to a vectorial sum of E_0 and E':

$$E = E_0 + E' \tag{8}$$

Based on above analysis, we can see that when the debris go through the coaxial cylindrical capacitive sensor, the original electric field of the sensor is changed because of the polarization effect, and this change further led to the capacitance change.

3. Numerical simulation

As discussed in Section 2, the capacitive sensor is a kind of capacitor with variable parameters (Itomi, 2006). When the inner core length and the distance between two electrodes are constant, the variation in the dielectric constant will change the capacitance value. To obtain better values of different parameters of capacitive sensor, it is necessary to understand the influence of the length and the distance on the sensor performance. The numerical simulations are carried on by the Ansys finite element software. Intelligent grid control method is adopted in the simulation, and the accuracy of the grid is adjusted by "size smart".

3.1 Parametric analysis of capacitive sensor for lubricant oil without debris

In the basis of simulation, we mainly focus on the sensor's length, the distance between two electrodes (cylinder surfaces) and the applied voltage. According to the formula (5), we can know that the sensor length has no influence on the electric field in the sensor. If the distance and the voltage between two electrodes are selected as control variables, the electric field in the sensor will be changed obviously. The simulations are carried out with different values of the distance and voltage. The dielectric of simulated capacitor is 80. The experiments fix R_1 = 1 mm, l = 40 mm as constant. There are two cases for simulation. The distance is set as 2, 3 and 4 mm, respectively, while keep the applied voltage U = 2 V; The voltage is set as 0.5,1 and 2 V, while keep the distance = 3 mm. After dividing the grid, there are 237222 nodes, 166057 units. The simulation results are shown in Figures 4 and 5.

Figure 4 The electric field distribution with different distances between two poles

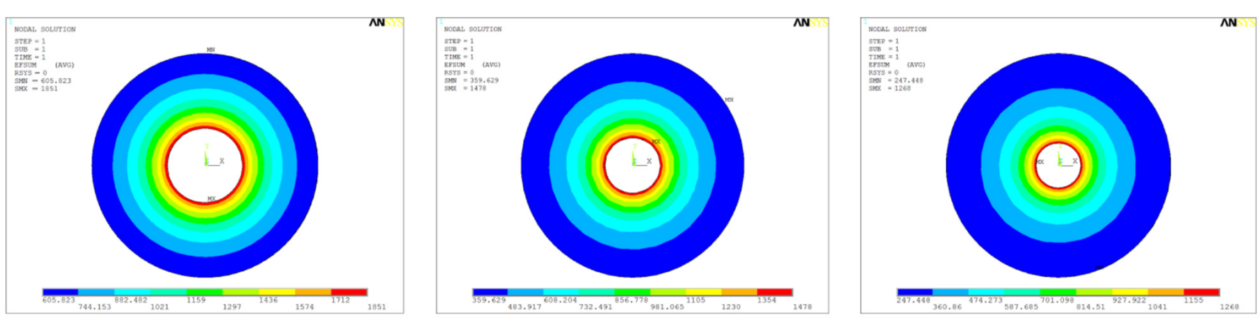

(a) (b) (c)

Notes: (a) Distance = 2 mm; (b) distance = 3 mm; (c) distance = 4 mm

Figure 5 The electric field distribution with different voltages

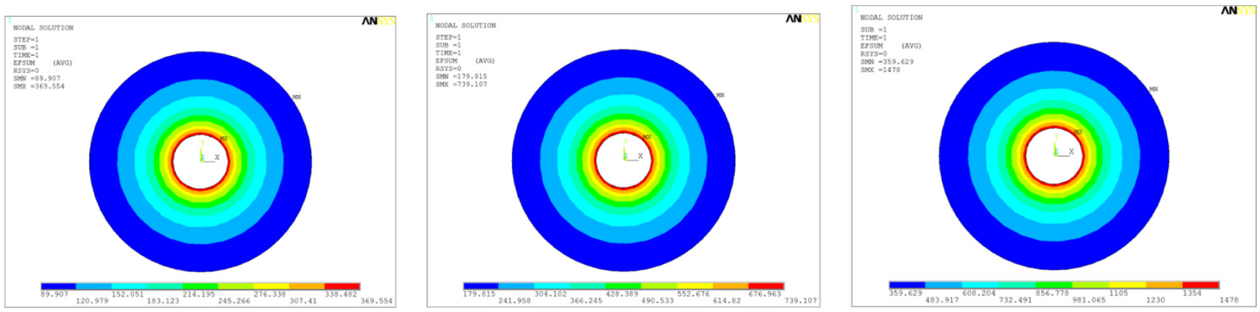

(a) (b) (c)

Notes: (a) Voltage = 0.5 V; (b) voltage = 1 V; (c) voltage = 2 V

Figure 6 The fitting result of different parameters

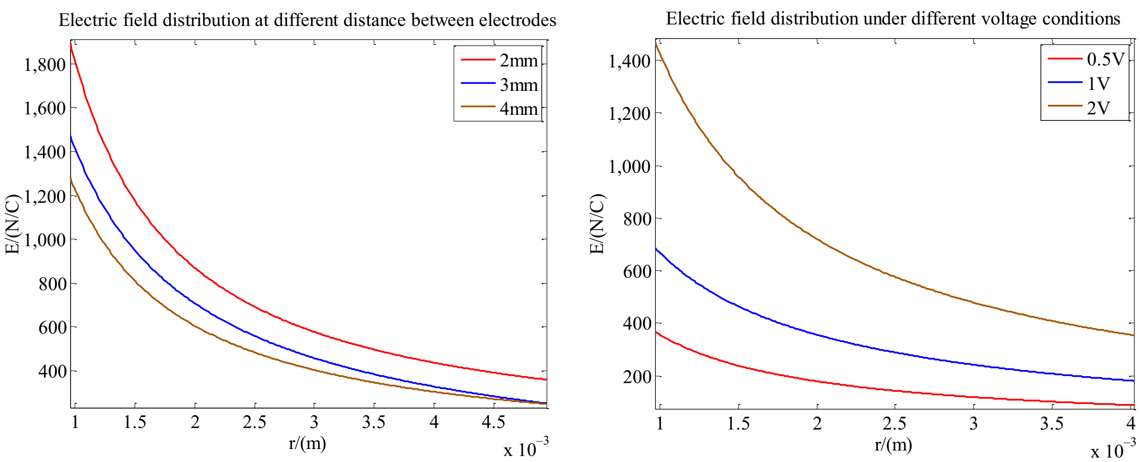

(a) (b)

Notes: (a) Different distances; (b) different voltages

In Figures 4 and 5, it is difficult to distinguish the difference in a way of quantitative comparison. So, we extract the simulation data and deal with these data using fitting method. The fitting results are shown in Figures 6(a) and 6(b). The relationship between the distance and the electric field intensity is illustrated in Figure 6(a). It is obviously found that the electric field intensity decreases with the increase of the distance between the two electrodes. The result indicates that there is an inverse proportion relation between them, which correlates well with equation (8). According to Figure 6(b), it can be seen that the greater the voltage applied between the two electrodes, the electric field strength of the sensor will be increased; meanwhile, the effect is more obvious at the early stage. Taking into account the effect of signal to noise ratio and the flow reduction, we set the distance between two electrodes as 3 mm and the applied voltage as 2 V.

Finally, to further verify the consistency between theoretical analysis and numerical simulation, we can compare the theoretical function (8) and the fitting curve of the data which extract from simulation. The comparison between these two

Figure 7 Comparison of theoretical function and simulation fitting curve

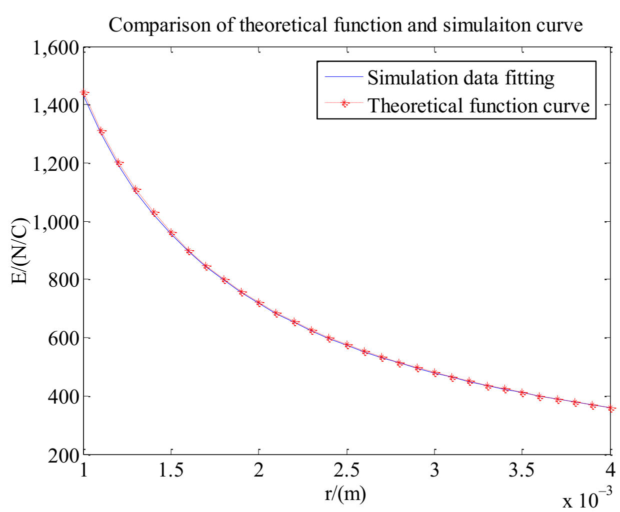

Figure 8 The electric field distribution with different number of debris

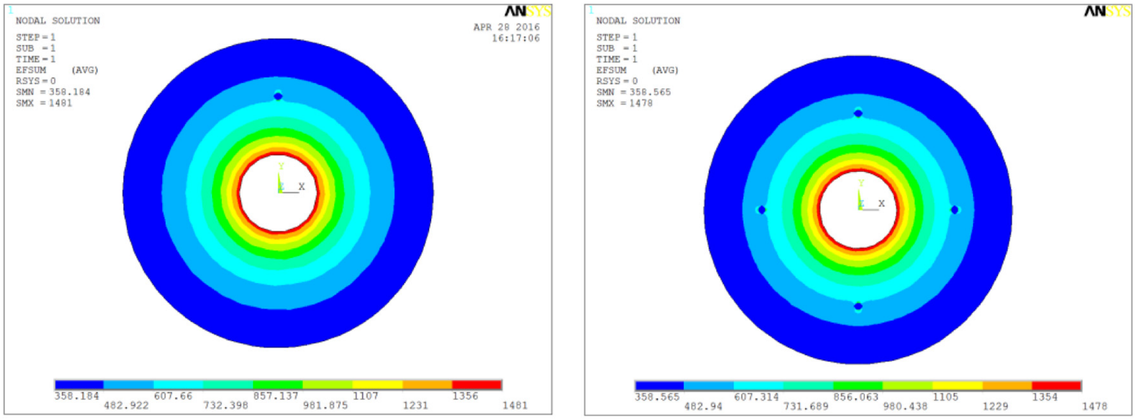

(a) (b)

Notes: (a) One debris; (b) four debris

Figure 9 The smooth curve of the electric field strength at different positions in two cases with one debris and without debris, respectively

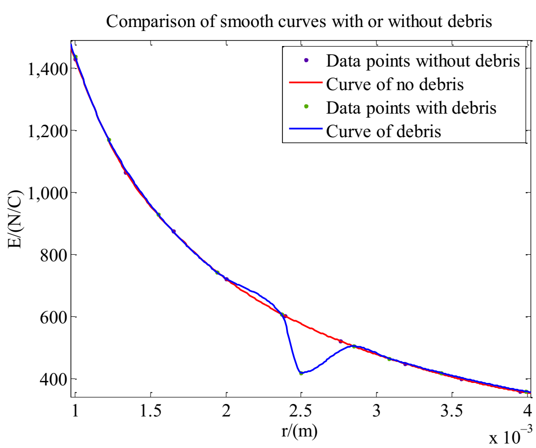

curves is shown in Figure 7. Apparently, these two cures are well consistent.

3.2 Electric field simulation of oil with debris

Based on the parametric analysis of above simulation, we can determine the values of different parameters of the presented sensor, i.e. the radius of the inner core is 1 mm; the distance between two electrodes is 3 mm; the length is 40 mm, and the applied voltage is 2 V. The electric fields of the sensor containing different numbers of debris are simulated and their results are shown in Figures 8(a) and 8(b). There is one debris and four debris in these two figures, respectively. From the simulation result, we can notice that the electric field distribution will be locally changed when the debris come into the sensor.

To compare the change of electric field strength for two cases (one debris and no debris), we extract the data at 15 points (the mesh nodes in the same element model) in two cases,

Figure 11 Experimental setup

(a) (b)

Notes: (a) Experimental equipment; (b) illustration of debris falling into sensor

Figure 10 Three components of the developed capacitive sensor

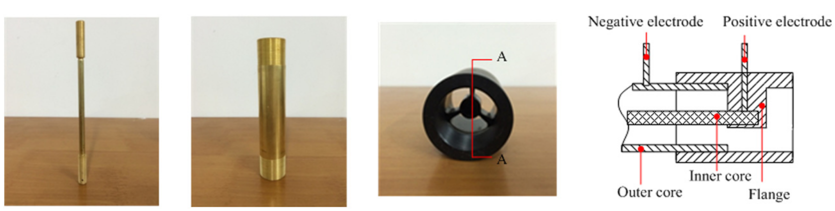

(a) (b) (c) (d)

Notes: (a) The inner core; (b) the outer core; (c) the flange; (d) assembly drawing in A-A section respectively. Two interpolation curves are illustrated in Figure 9. It is shown that the electric field strength decreases at the position where debris exists. It is easy to calculate that the simulation sensitivity is about 30 per cent.

Table I The change of the capacitance with the frequency in different medium (air, water and oil)

Frequency (Hz)	Capacitance (pF)/air	Capacitance (pF)/water	Capacitance (pF)/oil
100	10.13	1.9120e6	18.42
120	10.04	1.6568e6	18.35
150	9.94	1.3374e6	18.34
200	9.88	1.0215e6	18.30
400	9.75	0.5267e6	18.28
600	9.71	0.3396e6	18.16
800	9.66	0.2393e6	17.60
1,000	9.55	0.1783e6	16.43

4. Experiments

4.1 Experiment setup

The corresponding experiments are designed to verify the presented theoretical and numerical model. The inner and outer core material of the capacitive sensor is copper; the length is 40 mm; the inner core radius is 1 mm, and the distance between the two electrodes is 3 mm. The object is shown as Figures 10(a) and 10(b). To make the sensor easier to experiment, we design a plastic coaxial flange as shown in Figure 10(c). Two flanges are used to connect two coaxial cores. From the outer wall of flange to the inner core, there is a small hole used to install a metal conductive rod as shown in Figure 9(d). The external voltage is applied to the inner core by this electrode.

In the experiment, we used the measuring instrument LCR (LCR-8110G). With the LCR, we can directly apply voltage to the sensor and measure the capacitive. The chosen oil is SAE30, and the debris used in the debris monitoring experiments are iron debris. The experimental setup is shown in Figure 11.

Figure 12 The curve of the change of the capacitance with the frequency in different medium

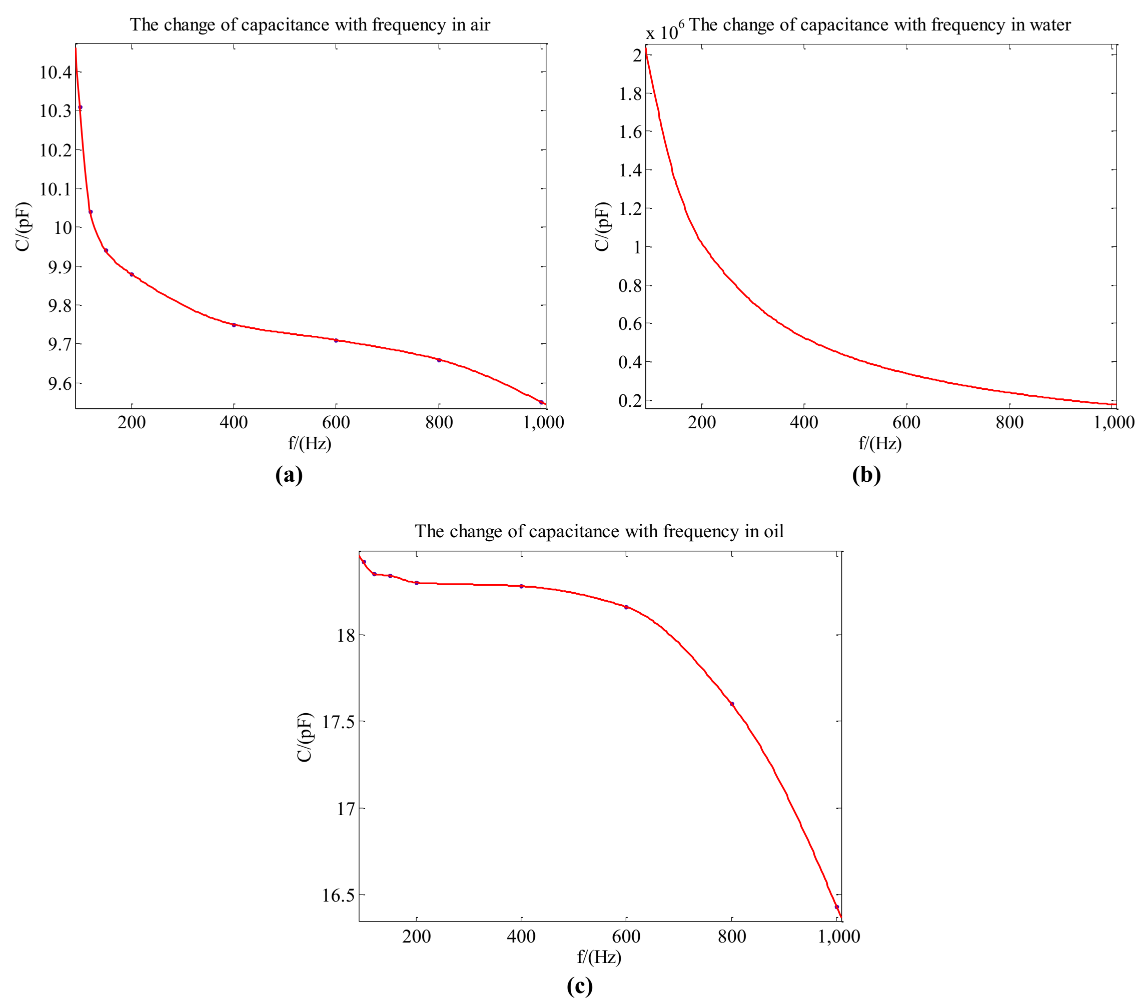

Notes: (a) Air; (b) water; (c) oil

Table II The measured capacitance for different number of debris in water or oil

No.	Capacitance (pF)/water	Capacitance (pF)/oil
0	1.9065e6	18.26
1	1.9285e6	18.36
2	1.9305e6	x
3	1.9422e6	19.15
5	1.9514e6	19.44
7	x	19.83
8	1.9655e6	x
9	1.9724e6	20.27
11	1.9830e6	x
13	2.0166e6	x
16	2.0226e6	x

Note: x means a large fluctuated capacitance value

4.2 Frequency selection

The simulation in Section 2 has confirmed that the voltage used in the experiment is 2 V, but the voltage frequency still needs to be further determined. In this section, the frequency is selected as a variable with different values, i.e. 100 Hz, 120 Hz, 150 Hz, 200 Hz, 400 Hz, 600 Hz, 800 Hz and 1,000 Hz. It is found that the measured sensor capacitances change with the frequency, when the medium is air, water, oil, respectively. The experiment data are shown in Table I. The corresponding curves of Table I are shown in Figures 12(a), 12(b) and 12(c).

It can be seen from Table I that the capacitance values of the sensor containing different medium show a trend of gradually decreasing with the increase of frequency. In actual measurement, the greater frequency is, the greater fluctuation of the capacitance value is. Therefore, the final values in Table I are average ones of three measured results. Although the capacitances of the sensor with different medium are generally decreased when the excited frequency increase, their change trends are not exactly same. From Figure 12, we can see that when the medium is air or water, their decline trends are roughly similar, but the trend in case of oil is completely different, the value is reduced slowly from 100 to 600 Hz, while rapidly increased in the range of high frequency. These different trends are caused by different viscosity of medium. To gain a stable value, the frequency 100 Hz is selected as the final value.

4.3 Debris monitoring

The series of experiments are carried out to illustrate the feasibility of the presented sensor. The experimental parameters are listed as follows: the applied voltage 2 V, the voltage frequency 100 Hz, three kinds of medium (air, water and oil) and the metal debris. The first experiment is to verify the sensor sensitivity to the number of the metal debris with the same size 1 mm × 1 mm × 0.5 mm. The second experiment is to show the effect of the debris size on the capacitance. The debris falls into the capacitance sensor with water or oil in the form of free fall from the 50 mm distance to the top of sensor, as shown in Figure 10(b). Therefore, the debris will fall into the sensor at a velocity to simulate the motion of fluid containing debris, although the actual liquid is static. As the viscosity of air is too low, the time that debris goes through the sensor in free fall is too short that there is no enough time for LCR reaction. Because of the high viscosity of water and oil, there is enough time that the debris goes through the sensor. So, the current tests are only concerned about water and oil in this section.

Table III The change of capacitance value with the debris size in water or oil

Size(mm)	Capacitance (pF)/water	Capacitance (pF)/oil
0	2.2855e6	18.17
3*1*0.5	2.3097e6	19.07
5*1*0.5	2.3435e6	19.43
7*1*0.5	2.3599e6	19.96
9*1*0.5	2.3759e6	x

Note: x means no capacitance value

Figure 13 The curves of the capacitance value with the number of debris in water or oil

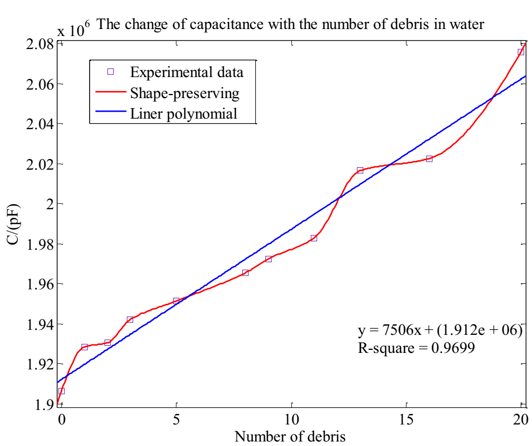

(a)

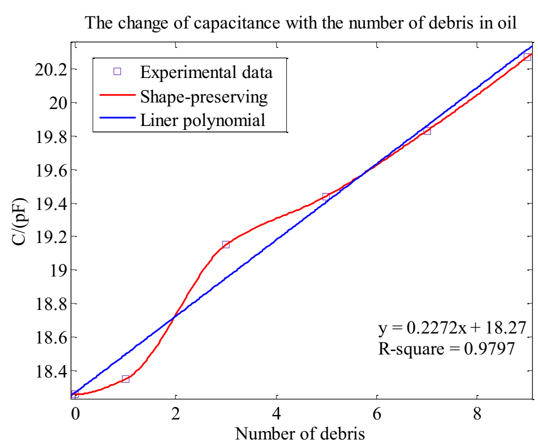

(b)

Notes: (a) Water; (b) oil

Figure 14 The trend on the change of the capacitance

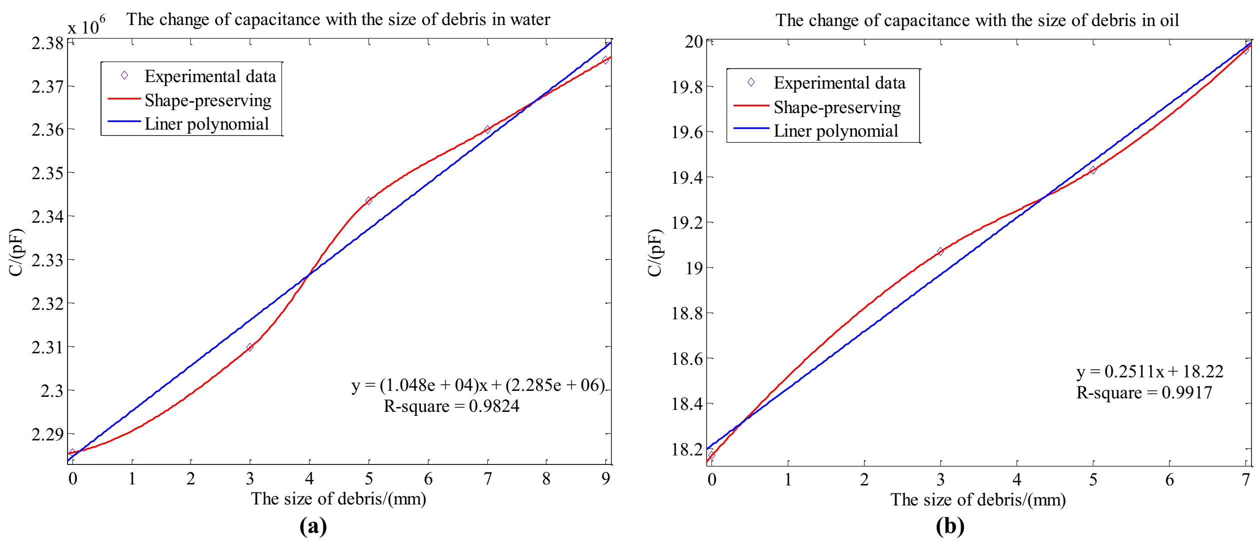

Notes: (a) Water; (b) oil

The results of the first experiment are shown in Table II. It can be seen that when the medium is water, the capacitance values of the presented sensor are much larger than those of sensor with the medium because of the good conductivity of water. With the increase of the debris number, the capacitance value increases with the increase of debris whether the medium is water or oil. The data of Table II are drawn into two curves as shown in Figure 13. We can see that the capacitance value is roughly linearly increased with the debris number, no matter the medium is water or oil. When a debris flows into the sensor, the capacitance will increase because the debris change the dielectric of the medium, which is corresponding to the result of simulation in Figure 9.

The results of the second experiment are listed in Table III to illustrate the influence of the debris size on the capacitance of the presented sensor with water and oil, respectively. The sizes of debris are different in the length, while the width and the thickness keep constant. These data are drawn into two curves to show the change trend of the capacitance value with the debris size, as shown in Figures 14(a) and 14(b). It can be seen that the capacitance is approximately linearly changed with the debris size. The linearity shown in different number and size of debris illustrates that the capacitance will linearly affected by debris, which means that the capacitance will linearly influenced by the change of dielectric.

5. Conclusions

Lubricant oil monitoring is an important part of aircraft engine health monitoring. The health state of engine can be characterized by means of the oil debris monitoring. This paper presents a new capacitive sensor structure based on two coaxial cylinders, which is suitable for *in situ* monitoring debris in the lubricant oil. The coaxial cylinder sensor is designed based on the variable dielectric constant caused by the debris. Meanwhile, the mathematical model is developed in two dimensions to describe the sensing mechanism and some relative sensors parameters. The results presented in this paper show that the sensor can detect the debris of lubricant oil in terms of electric field strength through simulation verification. Also, the experiment verifies that the proposed sensor configuration can characterize the debris in a way of capacitance values. Several experimental results indicate the developed capacitive sensor is sensitive to both size and number of debris. It is founded that the capacitance values increase almost linearly when the number and size of debris increase. However, there are lots of further works to do to apply the presented method into the application. Especially, it is necessary to consider several factors' influence on monitoring results. These factors include the flow rate of the lubricant oil, the temperature, the debris distribution and the vibration. Moreover, future work should consider the influence of the oil degradation to the capacitance change and other contaminations (e.g. water and dust).

References

Appleby, M., Choy, F., Du, I. and Zhe, J. (2013), "Oil debris and viscosity monitoring using ultrasonic and capacitance/inductance measurements", *Lubrication Science*, Vol. 25 No. 8, pp. 507-524.

Aslam, M.Z. and Tang, T.B. (2014), "A high resolution capacitive sensing system for the measurement of water content in crude oil", *Sensors (Basel, Switzerland)*, Vol. 14 No. 7, pp. 11351-11361.

Ding, X.Y., Zheng, H. and Jian, W.X. (2012), "Research on capacitive sensor for online oil monitoring", *Proceedings of Prognostics and System Health Management Conference (PHM-Shenzhen), IEEE*, pp. 1-4.

Dong, T. and Barbosa, C. (2015), "Capacitance variation induced by microfluidic two-Phase Flow across insulated interdigital electrodes in lab-on-Chip Devices", *Sensors (Basel, Switzerland)*, Vol. 15 No. 2, pp. 2694-2708.

Du, L., Carletta, J.E., Veillette, R.J. and Zhe, J. (2010), "Inductive coulter counting: Detection and differentiation of metal wear particles in lubricant", *Smart Materials and Structures*, Vol. 19 No. 5, p. 057001.

Du, L. and Zhe, J. (2011), "On-line wear debris detection in lubricating oil for condition based health monitoring of rotary machinery", *Recent Patents on Electrical Engineeringe)*, Vol. 4 No. 1, pp. 1-9.

Guan, L., Feng, X.L., Xiong, G. and Xie, J.A. (2011), "Application of dielectric spectroscopy for engine lubricating oil degradation monitoring", *Sensors and Actuators A*, Vol. 168 No. 1, pp. 22-29.

Hong, W., Wang, S., Tomovic, M.M., Liu, H. and Wang, X. (2015), "A new debris sensor based on dual excitation sources for online debris monitoring", *Measurement Science and Technology*, Vol. 26 No. 9.

Itomi, S. (2006), "Oil condition sensor", US Patent No.7112973, 2006-9-26.

Iwai, Y., Honda, T., Miyajima, T., Yoshinaga, S., Higashi, M. and Fuwa, Y. (2010), "Quantitative estimation of wear amounts by real time measurement of wear debris in lubricating oil", *Tribology International*, Vol. 43 Nos 1/2, pp. 388-394.

Jaw, L.C. (2005), "Recent advancements in aircraft engine health management (EHM) technologies and recommendations for the next step", ASME Turbo Expo 2005: Power for Land, Sea, and Air, *American Society of Mechanical Engineers*, 683-695.

Kayani, S.A. (2009), "Using combined XRD-XRF analysis to identify meteorite ablation debris", Int. Conf. on Islamabad, pp. 219-220.

Kuo, W.F., Chiou, Y.C. and Lee, R.T. (1997), "Fundamental characteristics of wear particle deposition measurement by an improved on-line ferrographic analyzer", *Wear*, Vol. 208 Nos 1/2, pp. 42-49.

Matsumoto, K., Tokunaga, T. and Kawabata, M. (2016), "Engine seizure monitoring system using wear debris analysis and particle measurement", SAE Technical Paper, 2016-01-0888, doi: 10.4271/2016-01-0888.

Mauntz, M.R., Gegner, J., Kuipers, U. and Klingau, S. (2013), "A sensor system for online oil condition monitoring of operating components", *Tribology – Fundamentals and Advancements*, chapter 11, IntechOpen, London, pp. 305-321.

Minasamudram, R., Agarwal, P. and Venkateswaran, P. (2013), "Simulation of a capacitive sensor for wear metal analysis of industrial oils", *Proceedings of the 2013 COMSOL Conference, Bangalore*.

Powrie, H. (2000), "Use of electrostatic technology for aero engine oil system monitoring", *Proceedings of Aerospace Conference, IEEE*, pp. 57-72.

Stevan, S.L. Jr., Paiter, L., Galvão, J.R., Roque, D.V. and Chaves, E.S. (2015), "Sensor and methodology for dielectric analysis of vegetal oils submitted to thermal stress", *Sensors*, Vol. 15 No. 10, pp. 26457-26477.

Wu, T., Wu, H., Du, Y. and Peng, Z. (2013), "Progress and trend of sensor technology for on-line oil monitoring", *Science China Technological Sciences*, Vol. 56 No. 12, pp. 2914-2926.

Wu, Y., Zhang, H., Zeng, L., Chen, H. and Sun, Y. (2016), "Determination of metal particles in oil using a microfluidic chip-based inductive sensor", *Instrumentation Science & Technology*, Vol. 44 No. 3, pp. 259-269.

Xu, C., Zhang, P., Wang, H., Li, Y. and Lv, C. (2015), "Ultrasonic echo waveshape features extraction based on QPSO-matching pursuit for online wear debris discrimination", *Mechanical Systems and Signal Processing*, Vols 60/61, pp. 301-315.

Zhang, H.P., Chon, C.H., Pan, X.X. and Li, D.Q. (2009), "Methods for counting particles in microfluidic applications", *Microfluidics and Nanofluidics*, Vol. 7 No. 6, pp. 739-749.

Corresponding author

Yishou Wang can be contacted at: wangys@xmu.edu.cn